

# Gravitational Wave Astronomy

Kostas D. Kokkotas

Theoretical Astrophysics, Auf der Morgenstelle 10,  
Eberhard Karls University of Tübingen, Tübingen 72076, Germany <sup>1</sup>

## Abstract

*As several large scale interferometers are beginning to take data at sensitivities where astrophysical sources are predicted, the direct detection of gravitational waves may well be imminent. This would open the gravitational-wave window to our Universe, and should lead to a much improved understanding of the most violent processes imaginable; the formation of black holes and neutron stars following core collapse supernovae and the merger of compact objects at the end of binary inspiral.*

## 1 Introduction

Gravitational waves are ripples of spacetime generated as masses are accelerated. It is one of the central predictions of Einstein's general theory of relativity but despite decades of effort these ripples in spacetime have still not been observed directly. Yet we have strong indirect evidence for their existence from the excellent agreement between the observed inspiral rate of the binary pulsar PSR1913+16 and the theoretical prediction (better than 1% in the phase evolution). This provides confidence in the theory and suggests that "gravitational-wave astronomy" should be viewed as a serious proposition. This new window onto universe will complement our view of the cosmos and will help us unveil the fabric of spacetime around black-holes, observe directly the formation of black holes or the merging of binary systems consisting of black holes or neutron stars, search for rapidly spinning neutron stars, dig deep into the very early moments of the origin of the universe, and look at the very center of the galaxies where supermassive black holes weighing millions of solar masses are hidden. Secondly, detecting gravitational waves is important for our understanding of the fundamental laws of physics; the proof that gravitational waves exist will verify a fundamental 90-year-old prediction of general relativity. Also, by comparing the arrival times of light and gravitational waves from, e.g., supernovae, Einstein's prediction that light and gravitational waves travel at the same speed could be checked. Finally, we could verify that they have the polarization predicted by general relativity.

These expectations follow from the comparison between gravitational and electromagnetic waves. That is : a) While electromagnetic waves are radiated by individual particles, gravitational waves are due to non-spherical bulk motion of matter. In essence, this means that the information carried by electromagnetic waves is stochastic in nature, while the gravitational waves provide insights into coherent mass currents. b) The electromagnetic waves will have been scattered many times. In contrast, gravitational waves interact weakly with matter and arrive at the Earth in pristine condition. This means that gravitational waves can be used to probe regions of space that are opaque to electromagnetic waves. Unfortunately, this weak interaction with matter also makes the detection of gravitational waves an extremely hard task. c) Standard astronomy is based on deep imaging of small fields of view, while gravitational-wave detectors cover virtually the entire sky. d) The wavelength of the electromagnetic radiation is smaller than the size of the emitter, while the wavelength of a gravitational wave is usually larger than the size of the source. This means that we cannot use gravitational-wave data to create an image of the source. In fact, gravitational-wave observations are more like audio than visual.

---

<sup>1</sup>Reviews in Modern Astrophysics, Vol 20, "Cosmic Matter", WILEY-VCH, Edited by S. Röser (2008)

## 2 Gravitational wave primer

The aim of the first part of our contribution is to provide a condensed text-book level introduction to gravitational waves. Although in no sense complete, this description should prepare the reader for the discussion of high-frequency sources which follows.

The first aspect of gravitational waves that we need to appreciate is their *tidal* nature. This is important because it implies that we need to monitor, with extreme precision, the relative motion of test masses or the periodic (tidal) deformations of extended bodies. A gravitational wave, propagating in a flat spacetime, generates periodic distortions, which can be described in terms of the Riemann tensor which measures the curvature of the spacetime. In linearized theory ( $h_{\mu\nu} \ll g_{\mu\nu}$ ) the Riemann tensor takes the following gauge-independent form:

$$R_{\kappa\lambda\mu\nu} = \frac{1}{2} (\partial_{\nu\kappa} h_{\lambda\mu} + \partial_{\lambda\mu} h_{\kappa\nu} - \partial_{\kappa\mu} h_{\lambda\nu} - \partial_{\lambda\nu} h_{\kappa\mu}), \quad (1)$$

which is considerably simplified by choosing the so called transverse and traceless gauge or *TT gauge*:

$$R_{j0k0}^{\text{TT}} = -\frac{1}{2} \frac{\partial^2}{\partial t^2} h_{jk}^{\text{TT}} \approx \frac{\partial^2 \Phi}{\partial x^j \partial x^k}, \quad j, k = 1, 2, 3. \quad (2)$$

where  $h_{jk}^{\text{TT}}$  is the gravitational wave field in the TT-gauge and  $\Phi$  describes the gravitational potential in Newtonian theory. The Riemann tensor is a pure geometrical object, but in general relativity has a simple physical interpretation: it is the tidal force field and describes the relative acceleration between two particles in free fall. If we assume two particles moving freely along geodesics of a curved spacetime with coordinates  $x^\mu(\tau)$  and  $x^\mu(\tau) + \delta x^\mu(\tau)$  (for a given value of the proper time  $\tau$ ,  $\delta x^\mu(\tau)$  is the displacement vector connecting the two events) it can be shown that, in the case of slowly moving particles,

$$\frac{d^2 \delta x^k}{dt^2} \approx -R^k{}_{0j0}{}^{\text{TT}} \delta x^j. \quad (3)$$

This is a simplified form of the equation of *geodesic deviation*. Hence, the tidal force acting on a particle is:

$$f^k \approx -m R^k{}_{0j0} \delta x^j, \quad (4)$$

where  $m$  is the mass of the particle. Equation (4) corresponds to the standard Newtonian relation for the tidal force acting on a particle in a field  $\Phi$ . Then equation (4) integrates to

$$\delta x_j = \frac{1}{2} h_{jk}^{\text{TT}} x_0^k \quad \text{or} \quad h \approx \frac{\Delta L}{L}, \quad (5)$$

where  $h$  is the dimensionless gravitational-wave strain.

Let us now assume that the waves propagate in the  $z$ -direction, i.e. that we have  $h_{jk} = h_{jk}(t - z)$ . Then one can show that we have only two independent components;

$$h_+ = h_{xx}^{\text{TT}} = -h_{yy}^{\text{TT}}, \quad h_\times = h_{xy}^{\text{TT}} = h_{yx}^{\text{TT}} \quad (6)$$

What effect does  $h_+$  have on matter? Consider a particle initially located at  $(x_0, y_0)$  and let  $h_\times = 0$  to find that

$$\delta x = \frac{1}{2} h_+ x_0 \quad \text{and} \quad \delta y = -\frac{1}{2} h_+ y_0. \quad (7)$$

That is, if  $h_+$  varies periodically then an object will first experience a stretch in the  $x$ -direction accompanied by a squeeze in the  $y$ -direction. One half-cycle later, the squeeze is in the  $x$ -direction and the stretch in the  $y$ -direction. It is straightforward to show that the effect of  $h_\times$  is the same, but rotated by 45 degrees. This is illustrated in Fig. 1. A general wave will be a linear combination of the two polarisations.

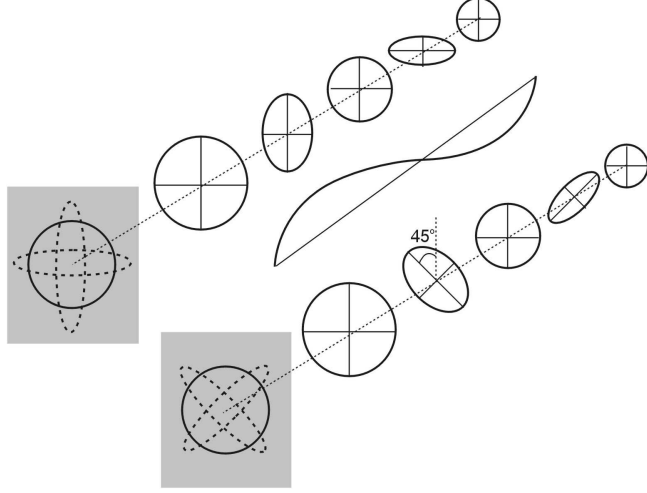


Figure 1: The effects of a gravitational wave travelling perpendicular the plane of a circular ring of particles, is sketched as a series of snapshots. The deformations due the two polarizations  $h_+$  and  $h_\times$  are shown.

Up to this point we have shown the effect of propagating spacetime deformations (we called them gravitational waves) on two nearby particles. But we have not yet done the connection to Einstein's theory. Thus we will describe with a tensor  $h_{\mu\nu}$  the variations of a flat spacetime from flatness, that is we will describe the spacetime with the metric  $g_{\alpha\beta} = \eta_{\alpha\beta} + h_{\alpha\beta}$ . Then after some algebra it can be shown that Einstein's equations will be reduced to the following form:

$$\left(-\frac{\partial^2}{\partial t^2} + \nabla^2\right) \tilde{h}^{\mu\nu} \equiv \partial_\lambda \partial^\lambda \tilde{h}^{\mu\nu} = 0 \quad \text{with} \quad \tilde{h}_{\mu\nu} \equiv h_{\mu\nu} - \frac{1}{2} \eta_{\mu\nu} h^\alpha{}_\alpha \quad (8)$$

where we have used a specific gauge choice  $\partial_\mu \tilde{h}^{\mu\nu} = 0$ , known as *Hilbert's gauge condition* (equivalent to the Lorentz gauge condition of electromagnetism).

The simplest solution to the wave equation (8) is a plane wave solution of the form

$$\tilde{h}^{\mu\nu} = A^{\mu\nu} e^{ik_\alpha x^\alpha}, \quad (9)$$

where  $A^{\mu\nu}$  is a constant symmetric tensor, the *polarization tensor*, in which information about the amplitude and the polarization of the waves is encoded, while  $k_\alpha$  is a constant vector, the *wave vector*, that determines the propagation direction of the wave and its frequency. In physical applications we will use only the real part of the above wave solution.

It is customary to write the gravitational wave solution in the TT gauge as  $h_{\mu\nu}^{TT}$ . That  $A_{\mu\nu}$  has only two independent components means that a gravitational wave is completely described by two dimensionless amplitudes,  $h_+$  and  $h_\times$ , say. If, for example, we assume a wave propagating along the z-direction, then the amplitude  $A^{\mu\nu}$  can be written as

$$A^{\mu\nu} = h_+ \epsilon_+^{\mu\nu} + h_\times \epsilon_\times^{\mu\nu} \quad (10)$$

where  $\epsilon_+^{\mu\nu}$  and  $\epsilon_\times^{\mu\nu}$  are the so-called *unit polarization tensors* defined by

$$\epsilon_+^{\mu\nu} \equiv \begin{pmatrix} 0 & 0 & 0 & 0 \\ 0 & 1 & 0 & 0 \\ 0 & 0 & -1 & 0 \\ 0 & 0 & 0 & 0 \end{pmatrix} \quad \epsilon_\times^{\mu\nu} \equiv \begin{pmatrix} 0 & 0 & 0 & 0 \\ 0 & 0 & 1 & 0 \\ 0 & 1 & 0 & 0 \\ 0 & 0 & 0 & 0 \end{pmatrix}. \quad (11)$$

Finally, we should point out that in the TT-gauge there is no difference between  $h_{\mu\nu}$  (the perturbation of the metric) and  $\tilde{h}_{\mu\nu}$  (the gravitational field).

## 2.1 Gravitational wave properties

Gravitational waves, once they are generated, propagate almost unimpeded. Indeed, it has been proven that they are even harder to stop than neutrinos! The only significant change they suffer as they propagate is the decrease in amplitude while they travel away from their source, and the *redshift* they feel (cosmological, gravitational or Doppler) as is the case for electromagnetic waves.

There are other effects that marginally influence the gravitational waveforms. For instance *absorption* by interstellar or intergalactic matter intervening between the observer and the source, which is extremely weak (actually, the extremely weak coupling of gravitational waves with matter is the main reason that gravitational waves have not been observed). *Scattering* and *dispersion* of gravitational waves are also practically unimportant, although they may have been important during the early phases of the universe (this is also true for the absorption). Gravitational waves can be *focused* by strong gravitational fields and also can be *diffracted*, exactly as it happens with the electromagnetic waves.

## 2.2 Energy flux carried by gravitational waves

Gravitational waves carry energy and cause a deformation of spacetime. The stress-energy carried by gravitational waves cannot be localized within a wavelength. Instead, one can say that a certain amount of stress-energy is contained in a region of the space which extends over several wavelengths. It can be proven that in the TT gauge of linearized theory the stress-energy tensor of a gravitational wave (in analogy with the stress-energy tensor of a perfect fluid) is given by

$$t_{\mu\nu}^{GW} = \frac{1}{32\pi} \langle \partial_\mu h_{ij}^{TT} \cdot \partial_\nu h_{ij}^{TT} \rangle. \quad (12)$$

where the angular brackets are used to indicate averaging over several wavelengths. For the special case of a plane wave propagating in the  $z$  direction, which we considered earlier, the stress-energy tensor has only three non-zero components, which take the simple form

$$t_{00}^{GW} = \frac{t_{zz}^{GW}}{c^2} = -\frac{t_{0z}^{GW}}{c} = \frac{1}{32\pi} \frac{c^2}{G} \omega^2 (h_+^2 + h_\times^2), \quad (13)$$

where  $t_{00}^{GW}$  is the energy density,  $t_{zz}^{GW}$  is the momentum flux and  $t_{0z}^{GW}$  the energy flow along the  $z$  direction per unit area and unit time (for practical reasons we have restored the normal units). The energy flux has all the properties one would anticipate by analogy with electromagnetic waves: (a) it is conserved (the amplitude dies out as  $1/r$ , the flux as  $1/r^2$ ), (b) it can be absorbed by detectors, and (c) it can generate curvature like any other energy source in Einstein's formulation of relativity.

The definition of the energy flux by equation (13) provides a useful formula

$$F = 3 \left( \frac{f}{1\text{kHz}} \right)^2 \left( \frac{h}{10^{-22}} \right)^2 \frac{\text{ergs}}{\text{cm}^2\text{sec}}, \quad (14)$$

which can be used to estimate the flux on Earth, given the amplitude of the waves (on Earth) and the frequency of the waves.

## 2.3 Generation of gravitational waves

As early as 1918, Einstein derived the quadrupole formula for gravitational radiation. This formula states that the wave amplitude  $h_{ij}$  is proportional to the second time derivative of the quadrupole moment of the source:

$$h_{ij} = \frac{2G}{r c^4} \ddot{Q}_{ij}^{TT} \left( t - \frac{r}{c} \right) \quad (15)$$

where

$$Q_{ij}^{TT}(x) = \int \rho \left( x^i x^j - \frac{1}{3} \delta^{ij} r^2 \right) d^3x \quad (16)$$

is the quadrupole moment in the TT gauge, evaluated at the retarded time  $t - r/c$  and  $\rho$  is the matter density in a volume element  $d^3x$  at the position  $x^i$ . This result is quite accurate for all sources, as long as the reduced wavelength  $\tilde{\lambda} = \lambda/2\pi$  is much longer than the source size  $R$ . It should be pointed out that the above result can be derived via a quite cumbersome calculation in which we solve the wave equation (8) with a source term  $T_{\mu\nu}$  on the right-hand side. In the course of such a derivation, a number of assumptions must be used. In particular, the observer must be located at a distance  $r \gg \tilde{\lambda}$ , far greater than the reduced wavelength, in the so called “radiation zone” and  $T_{\mu\nu}$  must not change very quickly.

Using the formulae (12) and (13) for the energy carried by gravitational waves, one can derive the luminosity in gravitational waves as a function of the third-order time derivative of the quadrupole moment tensor. This is the quadrupole formula

$$L_{GW} = -\frac{dE}{dt} = \frac{1}{5} \frac{G}{c^5} \left\langle \frac{\partial^3 Q_{ij}}{\partial t^3} \frac{\partial^3 Q_{ij}}{\partial t^3} \right\rangle. \quad (17)$$

Based on this formula, we derive some additional formulas, which provide order of magnitude estimates for the amplitude of the gravitational waves and the corresponding power output of a source. First, the quadrupole moment of a system is approximately equal to the mass  $M$  of the part of the system that moves, times the square of the size  $R$  of the system. This means that the third-order time derivative of the quadrupole moment is

$$\frac{\partial^3 Q_{ij}}{\partial t^3} \sim \frac{MR^2}{T^3} \sim \frac{Mv^2}{T} \sim \frac{E_{\text{ns}}}{T}, \quad (18)$$

where  $v$  is the mean velocity of the moving parts,  $E_{\text{ns}}$  is the kinetic energy of the component of the source’s internal motion which is non spherical, and  $T$  is the time scale for a mass to move from one side of the system to the other. The time scale (or period) is actually proportional to the inverse of the square root of the mean density of the system

$$T \sim \sqrt{R^3/GM}. \quad (19)$$

This relation provides a rough estimate of the characteristic frequency of the system  $f = 2\pi/T$ . For example, for a non-radially oscillating neutron star with a mass of roughly  $1.4M_\odot$  and a radius of 12km, the frequency of oscillation which is directly related to the frequency of the emitted gravitational waves, will be roughly 2kHz. Similarly, for an oscillating black hole of the same mass we get a characteristic frequency of 10kHz.

Then, the luminosity of gravitational waves of a given source is approximately

$$L_{GW} \approx \frac{G^4}{c^5} \left( \frac{M}{R} \right)^5 \sim \frac{G}{c^5} \left( \frac{M}{R} \right)^2 v^6 \sim \frac{c^5}{G} \left( \frac{R_{\text{Sch}}}{R} \right)^2 \left( \frac{v}{c} \right)^6 \quad (20)$$

and

$$h \approx \frac{1}{c^2} \left( \frac{GM}{r} \right) \left( \frac{R_{\text{Sch}}}{R} \right) \approx \frac{2}{c^2} \left( \frac{GM}{r} \right) \left( \frac{v}{c} \right)^2 \quad (21)$$

where  $R_{\text{Sch}} = 2GM/c^2$  is the Schwarzschild radius of the source. It is obvious that the maximum values of the amplitude and the luminosity of gravitational waves can be achieved if the source’s dimensions are of the order of its Schwarzschild radius and the typical velocities of the components of the system are of the order of the speed of light. This explains why we expect the best gravitational wave sources to be highly relativistic compact objects. The above formula sets also an upper limit on the power emitted by a source, which for  $R \sim R_{\text{Sch}}$  and  $v \sim c$  is

$$L_{GW} \sim c^5/G = 3.6 \times 10^{59} \text{ ergs/sec.} \quad (22)$$

This is an immense power, often called the *luminosity of the universe*.

Using the above order-of-magnitude estimates, we can get a rough estimate of the amplitude of gravitational waves at a distance  $r$  from the source:

$$h \sim \frac{G E_{\text{ns}}}{c^4 r} \sim \frac{G \varepsilon E_{\text{kin}}}{c^4 r} \quad (23)$$

where  $\varepsilon E_{\text{kin}}$  (with  $0 \leq \varepsilon \leq 1$ ), is the fraction of kinetic energy of the source that is able to produce gravitational waves. The factor  $\varepsilon$  is a measure of the asymmetry of the source and implies that only a time varying quadrupole moment will emit gravitational waves. For example, even if a huge amount of kinetic energy is involved in a given explosion and/or implosion, if the event takes place in a spherically symmetric manner, there will be no gravitational radiation.

Another formula for the amplitude of gravitational waves relation can be derived from the flux formula (14). If, for example, we consider an event (perhaps a supernovae explosion) at the Virgo cluster during which the energy equivalent of  $10^{-4} M_{\odot}$  is released in gravitational waves at a frequency of 1 kHz, and with signal duration of the order of 1 msec, the amplitude of the gravitational waves on Earth will be

$$h \approx 10^{-22} \left( \frac{E_{\text{GW}}}{10^{-4} M_{\odot} c^2} \right)^{1/2} \left( \frac{f}{1 \text{ kHz}} \right)^{-1} \left( \frac{\tau}{1 \text{ msec}} \right)^{-1/2} \left( \frac{r}{15 \text{ Mpc}} \right)^{-1}. \quad (24)$$

For a detector with arm length of 4 km we are looking for changes in the arm length of the order of

$$\Delta \ell = h \cdot \ell = 10^{-22} \cdot 4 \text{ km} = 4 \times 10^{-17} \text{ cm} !$$

This small number explains why all detection efforts till today were not successful.

If the signal analysis is based on matched filtering, the *effective amplitude* improves roughly as the square root of the number of observed cycles  $n$ . Using  $n \approx f\tau$  we get

$$h_c \approx 10^{-22} \left( \frac{E_{\text{GW}}}{10^{-3} M_{\odot} c^2} \right)^{1/2} \left( \frac{f}{1 \text{ kHz}} \right)^{-1/2} \left( \frac{r}{15 \text{ Mpc}} \right)^{-1} \quad (25)$$

We see that the “detector sensitivity” essentially depends only on the radiated energy, the characteristic frequency and the distance to the source. That is, in order to obtain a rough estimate of the relevance of a given gravitational-wave source at a given distance we only need to estimate the frequency and the radiated energy. Alternatively, if we know the energy released we can work out the distance at which these sources can be detected.

## 2.4 Gravitational wave detection

One often classifies gravitational-wave sources by the nature of the waves. This is convenient because the different classes require different approaches to the data-analysis problem;

- *Chirps*. As a binary system radiates gravitational waves and loses energy the two constituents spiral closer together. As the separation decreases the gravitational-wave amplitude increases, leading to a characteristic “chirp” signal.
- *Bursts*. Many scenarios lead to burst-like gravitational waves. A typical example would be black-hole oscillations excited during binary merger.
- *Periodic*. Systems where the gravitational-wave backreaction leads to a slow evolution (compared to the observation time) may radiate persistent waves with a virtually constant frequency. This would be the gravitational-wave analogue of the radio pulsars.
- *Stochastic*. A stochastic (non-thermal) background of gravitational waves is expected to have been generated following the Big Bang. One may also have to deal with stochastic gravitational-wave signals when the sources are too abundant for us to distinguish them as individuals.

Given that the weak signals are going to be buried in detector noise, we need to obtain as accurate theoretical models as possible. The rough order of magnitude estimates we just derived will certainly not be sufficient, even though they provide an indication as to whether it is worth spending the time and effort required to build a detailed model. Such source models are typically obtained using either

- Approximate perturbation techniques, eg. expansions in small perturbations away from a known solution to the Einstein equations, the archetypal case being black-hole and neutron star oscillations.
- Post-Newtonian approximations, essentially an expansion in the ratio between a characteristic velocity of the system and the speed of light, most often used to model the inspiral phase of a compact binary system.
- Numerical relativity, where the Einstein equations are formulated as an initial-value problem and solved on the computer. This is the only way to make progress in situations where the full nonlinearities of the theory must be included, eg. in the merger of black holes and neutron stars or a supernova core collapse.

The first attempt to detect gravitational waves was undertaken by the pioneer Joseph Weber during the early 1960s. He developed the first resonant mass (bar) detector and inspired many other physicists to build new detectors and to explore from a theoretical viewpoint possible cosmic sources of gravitational radiation. When a gravitational wave hits such a device, it causes the bar to vibrate. By monitoring this vibration, we can reconstruct the true waveform. The next step, was to monitor the change of the distance between two fixed points by a passing-by gravitational wave. This can be done by using laser interferometry. The use of interferometry is probably the most decisive step in our attempt to detect gravitational wave signals. Although the basic principle of such detectors is very simple, the sensitivity of detectors is limited by various sources of noise. The internal noise of the detectors can be Gaussian or non-Gaussian. The non-Gaussian noise may occur several times per day such as strain releases in the suspension systems which isolate the detector from any environmental mechanical source of noise, and the only way to remove this type of noise is via comparisons of the data streams from various detectors. The so-called Gaussian noise obeys the probability distribution of Gaussian statistics and can be characterized by a *spectral density*  $S_n(f)$ . The observed signal at the output of a detector consists of the true gravitational wave strain  $h$  and Gaussian noise. The optimal method to detect a gravitational wave signal leads to the following signal-to-noise ratio:

$$\left(\frac{S}{N}\right)_{\text{opt}}^2 = 2 \int_0^\infty \frac{|\tilde{h}(f)|^2}{S_n(f)} df, \quad (26)$$

where  $\tilde{h}(f)$  is the Fourier transform of the signal waveform. It is clear from this expression that the sensitivity of gravitational wave detectors is limited by noise.

In reality, the efficiency of a resonant bar detector depends on several other parameters. Here, we will discuss only the more fundamental ones. Assuming perfect isolation of the resonant bar detector from any external source of noise (acoustical, seismic, electromagnetic), the thermal noise is the only factor limiting our ability to detect gravitational waves. Thus, in order to detect a signal, the energy deposited by the gravitational wave every  $\tau$  seconds should be larger than the energy  $kT$  due to thermal fluctuations. This leads to a formula for the minimum detectable energy flux of gravitational waves, which, following equation (13), leads into a minimum detectable strain amplitude

$$h_{\text{min}} \leq \frac{1}{\omega_0 L Q} \sqrt{\frac{15kT}{M}} \quad (27)$$

where  $L$  and  $M$  are the size and the mass of the resonant bar correspondingly and  $Q$  is the quality factor of the material. During the last 20 years, a number of resonant bar detectors have

been in nearly continuous operation in several places around the world. They have achieved sensitivities of a few times  $10^{-21}$ , but still there has been no clear evidence of gravitational wave detection.

A laser interferometer is an alternative gravitational wave detector that offers the possibility of very high sensitivities over a broad frequency band. Originally, the idea was to construct a new type of resonant detector with much larger dimensions. Gravitational waves that are propagating perpendicular to the plane of the interferometer will increase the length of one arm of the interferometer, and at the same time will shorten the other arm, and vice versa. This technique of monitoring the waves is based on Michelson interferometry. L-shaped interferometers are particularly suited to the detection of gravitational waves due to their quadrupolar nature. For extensive reviews refer to [4, 5, 6, 7].

The US project named LIGO [8] (Laser Interferometer Gravitational Wave Observatory) consists of two detectors with arm length of 4 Km, one in Hanford, Washington, and one in Livingston, Louisiana. The detector in Hanford includes, in the same vacuum system, a second detector with arm length of 2 km. The detectors are already in operation and they achieved the designed sensitivity. The Italian/French EGO (VIRGO) detector [9] of arm-length 3 km at Cascina near Pisa is designed to have better sensitivity at lower frequencies. GEO600 is the German/British detector built in Hannover [10]. The TAMA300[11] detector in Tokyo has arm lengths of 300 m and it was the first major interferometric detector in operation. There are already plans for improving the sensitivities of all the above detectors and the construction of new interferometers in the near future.

Up to now LIGO has completed four science runs, S1 from August - September 2002, S2 from February - April 2003, S3 from October 2003 - January 2004, and S4 February - March 2005. These short science runs were interrupted with improvements which led LIGO to operate now with its designed sensitivity. The fifth science run, S5, (November 2005 - September 2007) surveyed a considerable larger volume of the Universe and set upper limits to a number of gravitational wave sources [13, 14, 15, 16, 17]. The “enhanced” LIGO interferometer is expected to commence an S6 science run in 2009 and will survey a volume of space eight times as great as the current LIGO. In 2011, the LIGO interferometers will be shut down for decommissioning in order to install advanced interferometers. With these advanced interferometers LIGO is expected to operate with ten times the current sensitivity which means a factor of 1000 increase in the volume of the Universe surveyed by 2014.

## 3 Sources of gravitational waves

### 3.1 Radiation from binary systems

Among the most interesting sources of gravitational waves are binaries. The inspiralling of such systems, consisting of black holes or neutron stars, is, as we will discuss later, the most promising source for the gravitational wave detectors. Binary systems are also the sources of gravitational waves whose dynamics we understand the best. They emit copious amounts of gravitational radiation, and for a given system we know quite accurately the amplitude and frequency of the gravitational waves in terms of the masses of the two bodies and their separation.

The gravitational-wave signal from inspiraling binaries is approximately sinusoidal, with a frequency which is twice the orbital frequency of the binary. According to equation (17) the gravitational radiation luminosity of the system is

$$L^{\text{GW}} = \frac{32 G}{5 c^5} \mu^2 a^4 \Omega^6 = \frac{32 G^4}{5 c^5} \frac{M^3 \mu^2}{a^5}, \quad (28)$$

where  $\Omega$  is the orbital angular velocity,  $a$  is the distance between the two bodies,  $\mu = M_1 M_2 / M$  is the reduced mass of the system and  $M = M_1 + M_2$  is its total mass. In order to obtain the last part of the relation, we have used Kepler’s third law,  $\Omega^2 = GM/a^3$ . As the gravitating system



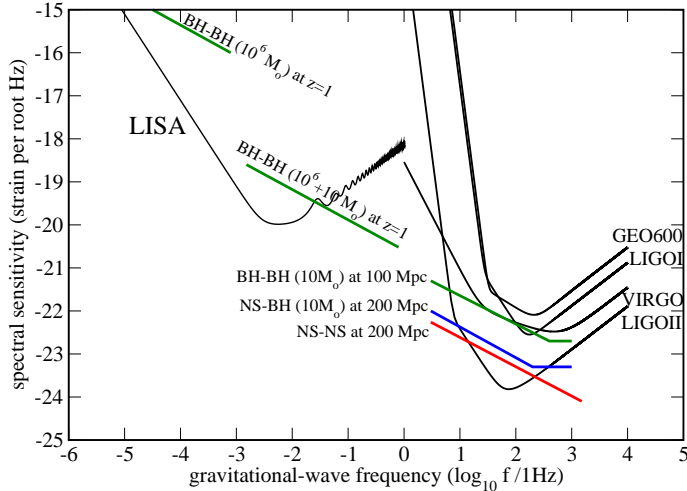


Figure 2: Estimated signal strengths for various inspiralling binaries relevant for ground- and space-based detectors.

loses energy by emitting radiation, the distance between the two bodies shrinks and the orbital frequency increases accordingly ( $\dot{T}/T = 1.5\dot{a}/a$ ). Finally, the amplitude of the gravitational waves is

$$h = 5 \times 10^{-22} \left( \frac{M}{2.8M_{\odot}} \right)^{2/3} \left( \frac{\mu}{0.7M_{\odot}} \right) \left( \frac{f}{100\text{Hz}} \right)^{2/3} \left( \frac{15\text{Mpc}}{r} \right). \quad (29)$$

In all these formulae we have assumed that the orbits are circular.

As the binary system evolves the orbit shrinks and the frequency increases in the characteristic chirp. Eventually, depending on the masses of the binaries, the frequency of the emitted gravitational waves will enter the bandwidth of the detector at the low-frequency end and will evolve quite fast towards higher frequencies. A system consisting of two neutron stars will be detectable by LIGO when the frequency of the gravitational waves is  $\sim 10\text{Hz}$  until the final coalescence around  $1\text{kHz}$ . This process will last for about  $15\text{min}$  and the total number of observed cycles will be of the order of  $10^4$ , which leads to an enhancement of the detectability by a factor 100 (remember  $h_c \sim \sqrt{nh}$ ). Binary neutron star systems and binary black hole systems with masses of the order of  $50M_{\odot}$  are the primary sources for LIGO. Given the anticipated sensitivity of LIGO, binary black hole systems are the most promising sources and could be detected as far as  $200\text{Mpc}$  away. For the present estimated sensitivity of LIGO the event rate is probably a few per year, but future improvements of detector sensitivity (the LIGO II phase) could lead to the detection of at least one event per month. Supermassive black hole systems of a few million solar masses are the primary source for LISA. These binary systems are rare, but due to the huge amount of energy released, they should be detectable from as far away as the boundaries of the observable universe. Finally, the recent discovery of the highly relativistic binary pulsar J0737-3039 [18] enhanced considerably the expected coalescence event rate of NS-NS binaries [19]. The event rate for initial LIGO is in the best case 0.2 per year while advanced LIGO might be able to detect 20-1000 events per year.

Depending on the high-density EOS and their initial masses, the outcome of the merger of two neutron stars may not always be a black hole, but a hypermassive, differentially rotating compact star (even if it is only temporarily supported against collapse by differential rotation). A recent detailed simulation[20] in full GR has shown that the hypermassive object created in a binary NS merger is nonaxisymmetric. The nonaxisymmetry lasts for a large number of rotational periods, leading to the emission of gravitational waves with a frequency of  $3\text{kHz}$  and

an effective amplitude of  $\sim 6 - 7 \times 10^{-21}$  at a large distance of 50Mpc. Such large effective amplitude may be detectable even by LIGO II at this high frequency.

The tidal disruption of a NS by a BH [21] or the merging of two NSs [22] may give valuable information for the radius and the EoS if we can recover the signal at frequencies higher than 1 kHz.

### 3.2 Gravitational collapse

One of the most spectacular astrophysical events is the core collapse of massive stars, leading to the formation of a neutron star (NS) or a black hole (BH). The outcome of core collapse depends sensitively on several factors: mass, angular momentum and metallicity of progenitor, existence of a binary companion, high-density equation of state, neutrino emission, magnetic fields, etc. Partial understanding of each of the above factors is emerging, but a complete and consistent theory for core collapse is still years away.

Roughly speaking, isolated stars more massive than  $\sim 8 - 10M_{\odot}$  end in core collapse and  $\sim 90\%$  of them are stars with masses  $\sim 8 - 20M_{\odot}$ . After core bounce, most of the material is ejected and if the progenitor star has a mass  $M \lesssim 20M_{\odot}$  a neutron star is left behind. On the other hand, if  $M \gtrsim 20M_{\odot}$  fall-back accretion increases the mass of the formed proton-neutron star (PNS), pushing it above the maximum mass limit, which results in the formation of a black hole. Furthermore, if the progenitor star has a mass of roughly  $M \gtrsim 45M_{\odot}$ , no supernova explosion is launched and the star collapses directly to a BH[23].

The above picture is, of course, greatly simplified. In reality, the metallicity of the progenitor, the angular momentum of the pre-collapse core and the presence of a binary companion will decisively influence the outcome of core collapse[24]. Rotation influences the collapse by changing dramatically the properties of the convective region above the proto-neutron star core. Centrifugal forces slow down infalling material in the equatorial region compared to material falling in along the polar axis, yielding a weaker bounce. This asymmetry between equator and poles also strongly influences the neutrino emission and the revival of the stalled shock by neutrinos [25, 26].

The supernova event rate is 1-2 per century per galaxy [27] and about 5-40% of them produce BHs in delayed collapse (through fall-back accretion), or direct collapse[28].

Of considerable importance is the *initial rotation rate* of proto-neutron stars, since (as will be detailed in the next sections) most mechanisms for emission of detectable gravitational waves from compact objects require very rapid rotation at birth (rotational periods of the order of a few milliseconds or less). Since most massive stars have non-negligible rotation rates (some even rotate near their break-up limit), simple conservation of angular momentum would suggest a proto-neutron star to be strongly differentially rotating with very high rotation rates and this picture is supported by numerical simulations of rotating core collapse[29, 30].

Other ways to form a rapidly rotating proto-neutron star would be through *fall-back accretion*[33], through the *accretion-induced collapse of a white dwarf* [34, 35, 36, 37] or through the merger of binary white dwarfs in globular clusters[38]. It is also relevant to take into account current gamma-ray-burst models. The *collapsar* [39] model requires high rotation rates of a proto-black hole [32]. In addition, a possible formation scenario for magnetars involves a rapidly rotating PNS formed through the collapse of a very massive progenitor and some observational evidence is already emerging [40].

Gravitational waves from core collapse have a rich spectrum, reflecting the various stages of this event. The initial signal is emitted due to the *changing axisymmetric quadrupole moment* during collapse. In the case of neutron star formation, the quadrupole moment typically becomes larger, as the core spins up during contraction. In contrast, when a rapidly rotating neutron star collapses to form a Kerr black hole, the axisymmetric quadrupole moment first increases but is finally reduced by a large factor when the black hole is formed.

A second part of the gravitational wave signal is produced when gravitational collapse is halted by the stiffening of the equation of state above nuclear densities and the core bounces,

driving an outwards moving shock. The dense fluid undergoes motions with relativistic speeds ( $v/c \sim 0.2 - 0.4$ ) and a rapidly rotating proto-neutron star thus oscillates in several of its axisymmetric *normal modes of oscillation*. This quasi-periodic part of the signal could last for hundreds of oscillation periods, before being effectively damped. If, instead, a black hole is directly formed, then black hole quasinormal modes are excited, lasting for only a few oscillation periods. A combination of neutron star and black hole oscillations will appear if the proton-neutron star is not stable but collapses to a black hole.

In a rotating PNS, nonaxisymmetric processes can yield additional types of gravitational wave signals. Such processes are *dynamical instabilities*, *secular gravitational-wave driven instabilities* or *convection* inside the PNS and in its surrounding hot envelope. *Anisotropic neutrino emission* is accompanied by a gravitational wave signal. *Nonaxisymmetries* could already be present in the pre-collapse core and become amplified during collapse[41]. Furthermore, if there is persistent fall-back accretion onto a PNS or black hole, these can be brought into *ringing*.

Below, we discuss in more detail those processes which result in high frequency gravitational radiation.

### 3.2.1 Neutron star formation

Core collapse as a potential source of GWs has been studied for more than three decades (some of the most recent simulations can be found in [42, 43, 36, 30, 44, 49, 50, 51, 52, 53]). The main differences between the various studies are the progenitor models (slowly or rapidly rotating), equation of state (polytropic or realistic), gravity (Newtonian or relativistic) and neutrino emission (simple, sophisticated or no treatment). In general, the gravitational wave signal from neutron star formation is divided into a core bounce signal, a signal due to convective motions and a signal due to anisotropic neutrino emission.

The core bounce signal is produced due to rotational flattening and excitation of normal modes of oscillations, the main contributions coming from the axisymmetric quadrupole ( $l = 2$ ) and quasi-radial ( $l = 0$ ) modes (the latter radiating through its rotationally acquired  $l = 2$  piece). If detected, such signals will be a unique probe for the high-density EOS of neutron stars [54, 55]. The strength of this signal is sensitive to the available angular momentum in the progenitor core. If the progenitor core is rapidly rotating, then core bounce signals from Galactic supernovae ( $d \sim 10\text{kpc}$ ) are detectable even with the initial LIGO/Virgo sensitivity at frequencies  $\lesssim 1\text{kHz}$ . In the best-case scenario, advanced LIGO could detect signals from distances of 1Mpc, but not from the Virgo cluster ( $\sim 15\text{Mpc}$ ), where the event rate would be high. The typical GW amplitude from 2D numerical simulations [30, 44, 45, 47, 46, 48] for an observer located in the equatorial plane of the source is [51]

$$h \approx 9 \times 10^{-21} \varepsilon \left( \frac{10\text{kpc}}{d} \right), \quad (30)$$

where  $\varepsilon \sim 1$  is the normalized GW amplitude. For such rapidly rotating initial models, the total energy radiated in GWs during the collapse is  $\lesssim 10^{-6} - 10^{-8} M_{\odot} c^2$ . If, on the other hand, progenitor cores are slowly rotating (due to e.g. magnetic torques[31]), then the signal strength is significantly reduced, but, in the best case, is still within reach of advanced LIGO for galactic sources.

Normal mode oscillations, if excited in an equilibrium star at a small to moderate amplitude, would last for hundreds to thousands of oscillation periods, being damped only slowly by gravitational wave emission or viscosity. However, the PNS immediately after core bounce has a very different structure than a cold equilibrium star. It has a high internal temperature and is surrounded by an extended, hot envelope. Nonlinear oscillations excited in the core after bounce can penetrate into the hot envelope. Through this damping mechanism, the normal mode oscillations are damped on a much shorter timescale (on the order of ten oscillation periods), which is typically seen in the core collapse simulations mentioned above.

*Convection signal.* The post-shock region surrounding a PNS is convectively unstable to both low-mode and high-mode convection. Neutrino emission also drives convection in this region. The most realistic 2D simulations of core collapse to date [50] have shown that the gravitational wave signal from convection significantly exceeds the core bounce signal for slowly rotating progenitors, being detectable with advanced LIGO for galactic sources, and is detectable even for nonrotating collapse. For slowly rotating collapse, there is a detectable part of the signal in the high-frequency range of 700Hz-1kHz, originating from convective motions that dominate around 200ms after core bounce. Thus, if both a core bounce signal and a convection signal would be detected in the same frequency range, these would be well separated in time.

*Neutrino signal.* In many simulations the gravitational wave signature of anisotropic neutrino emission has also been considered [56, 57, 58]. This type of signal can be detectable by advanced LIGO for galactic sources, but the main contribution is at low frequencies for a slowly rotating progenitor [50]. For rapidly rotating progenitors, stronger contributions at high frequencies could be present, but would probably be buried within the high-frequency convection signal.

Numerical simulations of neutron star formation have gone a long way, but a fully consistent 3D simulation including relativistic gravity, neutrino emission and magnetic fields is still missing. The combined treatment of these effects might not change the above estimations by orders of magnitude but it will provide more conclusive answers. There are also issues that need to be understood such as pulsar kicks (velocities exceeding 1000 km/s) which suggest that in a fraction of newly-born NSs (and probably BHs) the formation process may be strongly asymmetric [59]. Better treatment of the microphysics and construction of accurate progenitor models for the angular momentum distributions are needed. All these issues are under investigation by many groups.

### 3.2.2 Black hole formation

The gravitational-wave emission from the formation of a Kerr BH is a sum of two signals: the *collapse signal* and the *BH ringing*. The collapse signal is produced due to the changing multipole moments of the spacetime during the transition from a rotating iron core or PNS to a Kerr BH. A uniformly rotating neutron star has an axisymmetric quadrupole moment given by[60]

$$Q = -a \frac{J^2}{M}, \quad (31)$$

where  $a$  depends on the equation of state and is in the range of 2 – 8 for  $1.4M_\odot$  models. This is several times larger in magnitude than the corresponding quadrupole moment of a Kerr black hole ( $a = 1$ ). Thus, the *reduction* of the axisymmetric quadrupole moment is the main source of the collapse signal. Once the BH is formed, it continues to oscillate in its axisymmetric  $l = 2$  quasinormal mode (QNM), until all oscillation energy is radiated away and the stationary Kerr limit is approached.

The numerical study of rotating collapse to BHs was pioneered by Nakamura[61] but first waveforms and gravitational-wave estimates were obtained by Stark and Piran[62]. These simulations we performed in 2D, using approximate initial data (essentially a spherical star to which angular momentum was artificially added). A new 3D computation of the gravitational wave emission from the collapse of unstable uniformly rotating relativistic polytropes to Kerr BHs[63] finds that the energy emitted is

$$\Delta E \sim 1.5 \times 10^{-6} (M/M_\odot), \quad (32)$$

significantly less than the result of Stark and Piran. Still, the collapse of an unstable  $2M_\odot$  rapidly rotating neutron star leads to a characteristic gravitational-wave amplitude  $h_c \sim 3 \times 10^{-21}$ , at a frequency of  $\sim 5.5$ kHz, for an event at 10kpc. Emission is mainly through the "+" polarization, with the "x" polarization being an order of magnitude weaker.

Whether a BH forms promptly after collapse or a delayed collapse takes place depends sensitively on a number of factors, such as the progenitor mass and angular momentum and the high-density EOS. The most detailed investigation of the influence of these factors on the outcome of collapse has been presented recently in [53], where it was found that shock formation increases the threshold for black hole formation by  $\sim 20 - 40\%$ , while rotation results in an increase of at most 25%.

### 3.2.3 Black hole ringing through fall-back

A black hole can form after core collapse if fall-back accretion increases the mass of the PNS above the maximum mass allowed by axisymmetric stability. Material falling back after the black hole is formed excites the black hole QNMs of oscillation. If, on the other hand, the black hole is formed directly through core collapse (without a core bounce taking place) then most of the material of the progenitor star is accreted at very high rates ( $\sim 1 - 2M_\odot/s$ ) into the hole. In such *hyper-accretion* the black hole's QNMs can be excited for as long as the process lasts and until the black hole becomes stationary. Typical frequencies of the emitted GWs are in the range 1-3kHz for  $\sim 3 - 10M_\odot$  BHs.

The frequency and the damping time of the oscillations for the  $l = m = 2$  mode can be estimated via the relations [64]

$$\sigma \approx 3.2\text{kHz } M_{10}^{-1} \left[ 1 - 0.63(1 - a/M)^{3/10} \right] \quad (33)$$

$$Q = \pi\sigma\tau \approx 2(1 - a)^{-9/20} \quad (34)$$

These relations together with similar ones either for the 2nd QNM or the  $l = 2, m = 0$  mode can uniquely determine the mass  $M$  and angular momentum parameter  $a$  of the BH if the frequency and the damping time of the signal have been accurately extracted [65, 66, 67]. The amplitude of the ring-down waves depends on the BH's initial distortion, i.e. on the nonaxisymmetry of the blobs or shells of matter falling into the BH. If matter of mass  $\mu$  falls into a BH of mass  $M$ , then the gravitational wave energy is roughly

$$\Delta E \gtrsim \varepsilon\mu c^2(\mu/M) \quad (35)$$

where  $\varepsilon$  is related to the degree of asymmetry and could be  $\varepsilon \gtrsim 0.01$  [68]. This leads to an effective GW amplitude

$$h_{\text{eff}} \approx 2 \times 10^{-21} \left( \frac{\varepsilon}{0.01} \right) \left( \frac{10\text{Mpc}}{d} \right) \left( \frac{\mu}{M_\odot} \right) \quad (36)$$

## 3.3 Rotational instabilities

If proto-neutron stars rotate rapidly, nonaxisymmetric *dynamical instabilities* can develop. These arise from non-axisymmetric perturbations having angular dependence  $e^{im\phi}$  and are of two different types: the *classical bar-mode* instability and the more recently discovered *low- $T/|W|$  bar-mode* and *one-armed spiral* instabilities, which appear to be associated to the presence of corotation points. Another class of nonaxisymmetric instabilities are *secular instabilities*, driven by dissipative effects, such as fluid viscosity or gravitational radiation.

### 3.3.1 Dynamical instabilities

The classical  $m = 2$  bar-mode instability is excited in Newtonian stars when the ratio  $\beta = T/|W|$  of the rotational kinetic energy  $T$  to the gravitational binding energy  $|W|$  is larger than  $\beta_{\text{dyn}} = 0.27$ . The instability grows on a dynamical time scale (the time that a sound wave needs to travel across the star) which is about one rotational period and may last from 1 to 100 rotations depending on the degree of differential rotation in the PNS.

The bar-mode instability can be excited in a hot PNS, a few milliseconds after core bounce, or alternatively, it could also be excited a few tenths of seconds later, when the PNS cools due to neutrino emission and contracts further, with  $\beta$  becoming larger than the threshold  $\beta_{\text{dyn}}$  ( $\beta$  increases roughly as  $\sim 1/R$  during contraction). The amplitude of the emitted gravitational waves can be estimated as  $h \sim MR^2\Omega^2/d$ , where  $M$  is the mass of the body,  $R$  its size,  $\Omega$  the rotation rate and  $d$  the distance of the source. This leads to an estimation of the GW amplitude

$$h \approx 9 \times 10^{-23} \left(\frac{\epsilon}{0.2}\right) \left(\frac{f}{3\text{kHz}}\right)^2 \left(\frac{15\text{Mpc}}{d}\right) M_{1.4} R_{10}^2. \quad (37)$$

where  $\epsilon$  measures the ellipticity of the bar,  $M_{1.4}$  is measured in units of  $1.4M_\odot$  and  $R$  is measured in units of 10km. Notice that, in uniformly rotating Maclaurin spheroids, the GW frequency  $f$  is twice the rotational frequency  $\Omega$ . Such a signal is detectable only from sources in our galaxy or the nearby ones (our Local Group). If the sensitivity of the detectors is improved in the kHz region, signals from the Virgo cluster could be detectable. If the bar persists for many ( $\sim 10$ -100) rotation periods, then even signals from distances considerably larger than the Virgo cluster will be detectable. Due to the requirement of rapid rotation, the event rate of the classical dynamical instability is considerably lower than the SN event rate.

The above estimates rely on Newtonian calculations; GR enhances the onset of the instability,  $\beta_{\text{dyn}} \sim 0.24$  [69, 70] and somewhat lower than that for large compactness (large  $M/R$ ). Fully relativistic dynamical simulations of this instability have been obtained, including detailed waveforms of the associated gravitational wave emission. A detailed investigation of the required initial conditions of the progenitor core, which can lead to the onset of the dynamical bar-mode instability in the formed PNS, was presented in [51]. The amplitude of gravitational waves due to the bar-mode instability was found to be larger by an order of magnitude, compared to the axisymmetric core collapse signal.

*Low- $T/|W|$  instabilities.* The *bar-mode* instability may be excited for significantly smaller  $\beta$ , if centrifugal forces produce a peak in the density off the source's rotational center [71]. Rotating stars with a high degree of differential rotation are also dynamically unstable for significantly lower  $\beta_{\text{dyn}} \gtrsim 0.01$  [72, 73]. According to this scenario the unstable neutron star settles down to a non-axisymmetric quasi-stationary state which is a strong emitter of quasi-periodic gravitational waves

$$h_{\text{eff}} \approx 3 \times 10^{-22} \left(\frac{R_{\text{eq}}}{30\text{km}}\right) \left(\frac{f}{800\text{Hz}}\right)^{1/2} \left(\frac{100\text{Mpc}}{d}\right) M_{1.4}^{1/2}. \quad (38)$$

The bar-mode instability of differentially rotating neutron stars is an excellent source of gravitational waves, provided the high degree of differential rotation that is required can be realized. One should also consider the effects of viscosity and magnetic fields. If magnetic fields enforce uniform rotation on a short timescale, this could have strong consequences regarding the appearance and duration of the dynamical nonaxisymmetric instabilities.

An  $m = 1$  *one-armed spiral* instability has also been shown to become unstable in PNS, provided that the differential rotation is sufficiently strong [71, 74]. Although it is dominated by a "dipole" mode, the instability has a spiral character, conserving the center of mass. The onset of the instability appears to be linked to the presence of corotation points [75] (a similar link to corotation points has been proposed for the low- $T/|W|$  bar mode instability [76, 77]) and requires a very high degree of differential rotation (with matter on the axis rotating at least 10 times faster than matter on the equator). The  $m = 1$  spiral instability was recently observed in simulations of rotating core collapse, which started with the core of an evolved  $20M_\odot$  progenitor star to which differential rotation was added [78]. Growing from noise level ( $\sim 10^{-6}$ ) on a timescale of 5ms, the  $m = 1$  mode reached its maximum amplitude after  $\sim 100$ ms. Gravitational waves were emitted through the excitation of an  $m = 2$  nonlinear harmonic at a frequency of  $\sim 800$ Hz with an amplitude comparable to the core-bounce axisymmetric signal.

### 3.3.2 Secular gravitational-wave-driven instabilities

In a nonrotating star, the forward and backward moving modes of same  $(l, |m|)$  (corresponding to  $(l, +m)$  and  $(l, -m)$ ) have eigenfrequencies  $\pm|\sigma|$ . Rotation splits this degeneracy by an amount  $\delta\sigma \sim m\Omega$  and both the prograde and retrograde modes are dragged forward by the stellar rotation. If the star spins sufficiently rapidly, a mode which is retrograde (in the frame rotating with the star) will appear as prograde in the inertial frame (a nonrotating observer at infinity). Thus, an inertial observer sees GWs with positive angular momentum emitted by the retrograde mode, but since the perturbed fluid rotates slower than it would in the absence of the perturbation, the angular momentum of the mode in the rotating frame is negative. The emission of GWs consequently makes the angular momentum of the mode increasingly negative, leading to the instability. A mode is unstable when  $\sigma(\sigma - m\Omega) < 0$ . This class of *frame-dragging instabilities* is usually referred to as Chandrasekhar-Friedman-Schutz [79, 80] (CFS) instabilities.

*f-mode instability.* In the Newtonian limit, the  $l = m = 2$  *f*-mode (which has the shortest growth time of all polar fluid modes) becomes unstable when  $T/|W| > 0.14$ , which is near or even above the mass-shedding limit for typical polytropic EOSs used to model uniformly rotating neutron stars. Dissipative effects (e.g. shear and bulk viscosity or mutual friction in superfluids) [81, 82, 83, 84] leave only a small instability window near mass-shedding, at temperatures of  $\sim 10^9$ K. However, relativistic effects strengthen the instability considerably, lowering the required  $\beta$  to  $\approx 0.06 - 0.08$  [85, 86] for most realistic EOSs and masses of  $\sim 1.4M_\odot$  (for higher masses, such as hypermassive stars created in a binary NS merger, the required rotation rates are even lower).

Since PNSs rotate differentially, the above limits derived under the assumption of uniform rotation are too strict. Unless uniform rotation is enforced on a short timescale, due to e.g. magnetic braking [87], the *f*-mode instability will develop in a differentially rotating background, in which the required  $T/|W|$  is only somewhat larger than the corresponding value for uniform rotation [88], but the mass-shedding limit is dramatically relaxed. Thus, in a differentially rotating PNS, the *f*-mode instability window is huge, compared to the case of uniform rotation and the instability can develop provided there is sufficient  $T/|W|$  to begin with.

The *f*-mode instability is an excellent source of GWs. Simulations of its nonlinear development in the ellipsoidal approximation [89] have shown that the mode can grow to a large nonlinear amplitude, modifying the background star from an axisymmetric shape to a differentially rotating ellipsoid. In this modified background the *f*-mode amplitude saturates and the ellipsoid becomes a strong emitter of gravitational waves, radiating away angular momentum until the star is slowed-down towards a stationary state. In the case of uniform density ellipsoids, this stationary state is the Dedekind ellipsoid, i.e. a nonaxisymmetric ellipsoid with internal flows but with a stationary (nonradiating) shape in the inertial frame. In the ellipsoidal approximation, the nonaxisymmetric pattern radiates gravitational waves sweeping through the LIGO II sensitivity window (from 1kHz down to about 100Hz) which could become detectable out to a distance of more than 100Mpc.

Two recent hydrodynamical simulations [90, 91] (in the Newtonian limit and using a post-Newtonian radiation-reaction potential) essentially confirm this picture. In [90] a differentially rotating,  $N = 1$  polytropic model with a large  $T/|W| \sim 0.2 - 0.26$  is chosen as the initial equilibrium state. The main difference of this simulation compared to the ellipsoidal approximation comes from the choice of EOS. For  $N = 1$  Newtonian polytropes it is argued that the secular evolution cannot lead to a stationary Dedekind-like state. Instead, the *f*-mode instability will continue to be active until all nonaxisymmetries are radiated away and an axisymmetric shape is reached. This conclusion should be checked when relativistic effects are taken into account, since, contrary to the Newtonian case, relativistic  $N = 1$  uniformly rotating polytropes *are* unstable to the  $l = m = 2$  *f*-mode [85] – however it is not possible to date to construct relativistic analogs of Dedekind ellipsoids.

In the other recent simulation [91], the initial state was chosen to be a uniformly rotating,  $N = 0.5$  polytropic model with  $T/|W| \sim 0.18$ . Again, the main conclusions reached in [89] are confirmed, however, the assumption of uniform initial rotation limits the available angular momentum that can be radiated away, leading to a detectable signal only out to about  $\sim 40$ Mpc. The star appears to be driven towards a Dedekind-like state, but after about 10 dynamical periods the shape is disrupted by growing short-wavelength motions, which are suggested to arise because of a shearing type instability, such as the elliptic flow instability [92].

*r-mode instability.* Rotation does not only shift the spectra of polar modes; it also lifts the degeneracy of axial modes, and gives rise to a new family of *inertial* modes, of which the  $l = m = 2$  *r*-mode is a special member. The restoring force for these oscillations is the Coriolis force. Inertial modes are primarily velocity perturbations. The frequency of the *r*-mode in the rotating frame of reference is  $\sigma = 2\Omega/3$ . According to the criterion for the onset of the CFS instability, the *r*-mode is unstable for any rotation rate of the star [93, 94]. For temperatures between  $10^7 - 10^9$ K and rotation rates larger than 5-10% of the Kepler limit, the growth time of the unstable mode is smaller than the damping times of the bulk and shear viscosity [95, 96]. The existence of a solid crust or of hyperons in the core [97] and magnetic fields [98, 99], can also significantly affect the onset of the instability (for extended reviews see [100, 101]). The suppression of the *r*-mode instability by the presence of hyperons in the core is not expected to operate efficiently in rapidly rotating stars, since the central density is probably too low to allow for hyperon formation. Moreover, a recent calculation [102] finds the contribution of hyperons to the bulk viscosity to be two orders of magnitude smaller than previously estimated. If accreting neutron stars in Low Mass X-Ray Binaries (LMXB, considered to be the progenitors of millisecond pulsars) are shown to reach high masses of  $\sim 1.8M_\odot$ , then the EOS could be too stiff to allow for hyperons in the core (for recent observations that support a high mass for some millisecond pulsars see [103]).

The unstable *r*-mode grows exponentially until it saturates due to nonlinear effects at some maximum amplitude  $\alpha_{max}$ . The first computation of nonlinear mode couplings using second-order perturbation theory suggested that the *r*-mode is limited to very small amplitudes (of order  $10^{-3} - 10^{-4}$ ) due to transfer of energy to a large number of other inertial modes, in the form of a cascade, leading to an equilibrium distribution of mode amplitudes [104]. The small saturation values for the amplitude are supported by recent nonlinear estimations [105, 106] based on the drift, induced by the *r*-modes, causing differential rotation. On the other hand, hydrodynamical simulations of limited resolution showed that an initially large-amplitude *r*-mode does not decay appreciably over several dynamical timescales [108]. However, on a somewhat longer timescale a catastrophic decay was observed [109] indicating a transfer of energy to other modes, due to nonlinear mode couplings and suggesting that a hydrodynamical instability may be operating. A specific resonant 3-mode coupling was identified [110] as the cause of the instability and a perturbative analysis of the decay rate suggests a maximum saturation amplitude  $\alpha_{max} < 10^{-2}$ . A new computation using second-order perturbation theory finds that the catastrophic decay seen in the hydrodynamical simulations [109, 110] can indeed be explained by a parametric instability operating in 3-mode couplings between the *r*-mode and two other inertial modes [111, 112, 113, 107]. Whether the maximum saturation amplitude is set by a network of 3-mode couplings or a cascade is reached, is, however, still unclear.

A neutron star spinning down due to the *r*-mode instability will emit gravitational waves of amplitude

$$h(t) \approx 10^{-21} \alpha \left( \frac{\Omega}{\text{kHz}} \right) \left( \frac{100\text{kpc}}{d} \right) \quad (39)$$

Since  $\alpha$  is small, even with LIGO II the signal is undetectable at large distances (VIRGO cluster) where the SN event rate is appreciable, but could be detectable after long-time integration from a galactic event. However, if the compact object is a strange star, then the instability may not reach high amplitudes ( $\alpha \sim 10^{-3} - 10^{-4}$ ) but it will persist for a few hundred years (due to the different temperature dependence of viscosity in strange quark matter) and in this case there might be up to ten unstable stars in our galaxy at any time [114]. Integrating data for a



few weeks could lead to an effective amplitude  $h_{\text{eff}} \sim 10^{-21}$  for galactic signals at frequencies  $\sim 700 - 1000\text{Hz}$ . The frequency of the signal changes only slightly on a timescale of a few months, so that the radiation is practically monochromatic.

**Other unstable modes.** The CFS instability can also operate for core g-mode oscillations [115] but also for  $w$ -mode oscillations, which are basically spacetime modes [116]. In addition, the CFS instability can operate through other dissipative effects. Instead of the gravitational radiation, any radiative mechanism (such as electromagnetic radiation) can in principle lead to an instability.

### 3.4 Accreting neutron stars in LMXBs

Spinning neutron stars with even tiny deformations are interesting sources of gravitational waves. The deformations might result from various factors but it seems that the most interesting cases are the ones in which the deformations are caused by accreting material. A class of objects called Low-Mass X-Ray Binaries (LMXB) consist of a fast rotating neutron star (spin  $\approx 270 - 650\text{Hz}$ ) torqued by accreting material from a companion star which has filled up its Roche lobe. The material adds both mass and angular momentum to the star, which, on timescales of the order of tenths of Megayears could, in principle, spin up the neutron star to its break up limit. One viable scenario [118] suggests that the accreted material (mainly hydrogen and helium) after an initial phase of thermonuclear burning undergoes a non-uniform crystallization, forming a crust at densities  $\sim 10^8 - 10^9\text{g/cm}^3$ . The quadrupole moment of the deformed crust is the source of the emitted gravitational radiation which slows-down the star, or halts the spin-up by accretion.

An alternative scenario has been proposed by Wagoner [119] as a follow up of an earlier idea by Papaloizou-Pringle [120]. The suggestion was that the spin-up due to accretion might excite the  $f$ -mode instability before the rotation reaches the breakup spin. The emission of gravitational waves will torque down the star's spin at the same rate as the accretion will torque it up, however, it is questionable whether the  $f$ -mode instability will ever be excited for old, accreting neutron stars. Following the discovery that the  $r$ -modes are unstable at any rotation rate, this scenario has been revived independently by Bildsten [118] and Andersson, Kokkotas and Stergioulas [121]. The amplitude of the emitted gravitational waves from such a process is quite small, even for high accretion rates, but the sources are persistent and in our galactic neighborhood the expected amplitude is

$$h \approx 10^{-27} \left( \frac{1.6\text{ms}}{P} \right)^5 \frac{1.5\text{kpc}}{D}. \quad (40)$$

This signal is within reach of advanced LIGO with signal recycling tuned at the appropriate frequency and integrating for a few months [1]. This picture is in practice more complicated, since the growth rate of the  $r$ -modes (and consequently the rate of gravitational wave emission) is a function of the core temperature of the star. This leads to a thermal runaway due to the heat released as viscous damping mechanisms counteract the  $r$ -mode growth [122]. Thus, the system executes a limit cycle, spinning up for several million years and spinning down in a much shorter period. The duration of the unstable part of the cycle depends critically on the saturation amplitude  $\alpha_{\text{max}}$  of the  $r$ -modes [123, 124]. Since current computations [104, 106] suggest an  $\alpha_{\text{max}} \sim 10^{-3} - 10^{-4}$ , this leads to a quite long duration for the unstable part of the cycle of the order of  $\sim 1\text{Myr}$ .

The instability window depends critically on the effect of the shear and bulk viscosity and various alternative scenarios might be considered. The existence of hyperons in the core of neutron stars induces much stronger bulk viscosity, which suggests a much narrower instability window for the  $r$ -modes and the bulk viscosity prevails over the instability, even in temperatures as low as  $10^8\text{K}$  [97]. A similar picture can be drawn if the star is composed of "deconfined"  $u$ ,  $d$  and  $s$  quarks - a strange star [125]. In this case, there is a possibility that the strange stars in LMXBs evolve into a quasi-steady state with nearly constant rotation rate, temperature

and mode amplitude [114] emitting gravitational waves for as long as the accretion lasts. This result has also been found later for stars with hyperon cores [126, 127]. It is interesting that the stalling of the spin up in millisecond pulsars (MSPs) due to  $r$ -modes is in good agreement with the minimum observed period and the clustering of the frequencies of MSPs [123].

### 3.5 Gravitational-wave asteroseismology

If various types of oscillation modes are excited during the formation of a compact star and become detectable by gravitational wave emission, one could try to identify observed frequencies with frequencies obtained by mode-calculations for a wide parameter range of masses, angular momenta and EoSs [55, 128, 129, 130, 131, 132]. Thus, *gravitational wave asteroseismology* could enable us to estimate the mass, radius and rotation rate of compact stars, leading to the determination of the "best-candidate" high-density EoS, which is still very uncertain. For this to happen, accurate frequencies for different mode-sequences of rapidly rotating compact objects have to be computed.

For slowly rotating stars, the frequencies of  $f$ -,  $p$ - and  $w$ - modes are still unaffected by rotation, and one can construct approximate formulae in order to relate observed frequencies and damping times of the various stellar modes to stellar parameters. For example, for the fundamental oscillation ( $l = 2$ ) mode ( $f$ -mode) of non-rotating stars one obtains [55]

$$\sigma(\text{kHz}) \approx 0.8 + 1.6M_{1.4}^{1/2}R_{10}^{-3/2} + \delta_1 m\bar{\Omega} \quad (41)$$

$$\tau^{-1}(\text{secs}^{-1}) \approx M_{1.4}^3 R_{10}^{-4} (22.9 - 14.7M_{1.4}R_{10}^{-1}) + \delta_2 m\bar{\Omega} \quad (42)$$

where  $\bar{\Omega}$  is the normalized rotation frequency of the star, and  $\delta_1$  and  $\delta_2$  are constants estimated by sampling data from various EOSs. The typical frequencies of NS oscillation modes are larger than 1kHz. Since each type of mode is sensitive to the physical conditions where the amplitude of the mode is largest, the more oscillations modes can be identified through gravitational waves, the better we will understand the detailed internal structure of compact objects, such as the existence of a possible superfluid state of matter [133].

If, on the other hand, some compact stars are born rapidly rotating with moderate differential rotation, then their central densities will be much smaller than the central density of a nonrotating star of the same baryonic mass. Correspondingly, the typical axisymmetric oscillation frequencies will be smaller than 1kHz, which is more favorable for the sensitivity window of current interferometric detectors [134]. Indeed, axisymmetric simulations of rotating core-collapse have shown that if a rapidly rotating NS is created, then the dominant frequency of the core-bounce signal (originating from the fundamental  $l = 2$  mode or the  $l = 2$  piece of the fundamental quasi-radial mode) is in the range 600Hz-1kHz [30].

If different types of signals are observed after core collapse, such as both an axisymmetric core-bounce signal and a nonaxisymmetric one-armed instability signal, with a time separation of the order of 100ms, this would yield invaluable information about the angular momentum distribution in the proto-neutron stars.

### Acknowledgements

I am grateful to N. Andersson, N. Stergioulas, P. Lasky and A. Colaiuda for suggestions which improved the original manuscript. This work was supported by the German Foundation (DFG) via SFB/TR7 and by the EU program ILIAS.

### References

- [1] Cutler C, Thorne K S 2002: *in proceedings of GR16 (Durban South Africa, 2001)*, gr-qc/0204090
- [2] Schnabel R, Harms J, Strain K A, Danzmann K 2004, *Class. Quantum Grav.* **21**, S1155

- [3] Bonaldi M, Cerdonio M, Conti L, Prodi G A, Taffarello L, Zendri J P : 2004 *Class. Quantum Grav.* **21**, S1155
- [4] Saulson P R, 1994 *Fundamentals of Interferometric Gravitational Wave Detectors*, World Scientific
- [5] Blair D. G., 1991, *The Detection of Gravitational Waves*, Cambridge University Press
- [6] Hough J and Rowan S 2000 *Gravitational Wave Detection by Interferometry (Ground and Space)*, *Living Rev. Relativity* **3** 1.
- [7] Maggiore M 2008 *Gravitational Waves*, Oxford
- [8] LIGO <http://www.ligo.caltech.edu>
- [9] VIRGO <http://www.pi.infn.it/virgo/virgoHome.html>
- [10] GEO <http://www.geo600.uni-hannover.de>
- [11] TAMA <http://tamago.mtk.nao.ac.jp>
- [12] LISA <http://lisa.jpl.nasa.gov>
- [13] By LIGO Collaboration (B. Abbott et al.) *Phys. Rev. Lett.* **95**: 221101,2005.
- [14] By LIGO Collaboration (B. Abbott et al.) *Phys. Rev. D* **72**: 082001,2007.
- [15] By LIGO Collaboration (B. Abbott et al.) *Phys. Rev. D* **73**: 062001,2007.
- [16] By LIGO Collaboration (B. Abbott et al.) *Astrophys.J.* **659**:918-930,2007.
- [17] By LIGO Collaboration (B. Abbott et al.) *Phys. Rev. D* **76**: 042001,2007.
- [18] Burgay M, D'Amico N, Possenti A, Manchester R N, Lyne A G, Joshi B C, McLaughlin M A, Kramer M, Sarkissian J M, Camilo F, Kalogera V, Kim C, Lorimer D R: 2003, *Nature*, **426**, 531
- [19] Kalogera V, Kim C, Lorimer D R, Burgay M, D'Amico N, Possenti A, Manchester R N, Lyne A G, Joshi B C, McLaughlin M A, Kramer M, Sarkissian J M, Camilo F : 2004 *Astrophys.J.* **601**, L179
- [20] Shibata M 2005 *Phys. Rev. Lett.* **94** 201101
- [21] Vallisneri M 2000 *Phys. Rev. Lett.* **84** 3519
- [22] Faber J A, Glandcment P, Rasio F A and Taniguchi K 2002 *Phys. Rev. Lett.* **89** 231102
- [23] Fryer C L 1999 *Astrophys. J.* **522** 413
- [24] Fryer C L 2003 *Class. Quantum Gravity* **20** S73
- [25] Fryer C L and Warren M S 2004 *Astrophys. J.* **601** 391
- [26] Burrows A, Walder R, Ott C D and Livne E 2005 *Nucl. Phys. A* **752** 570
- [27] Cappellaro E, Turatto M, Tsvetov D Yu, Bartunov O S, Pollas C, Evans R and Hamuy M 1999 *A&A* **351** 459
- [28] Fryer C L and Kalogera V 2001 *Asrophys.J* **554**, 548
- [29] Fryer C L and Heger A 2000 *Astrophys. J.* **541** 1033
- [30] Dimmelmeier H, Font J A and Müller E 2002 *A&A* **393** 523
- [31] Spruit H C 2002 *Astron. Astrophys.* **381** 923
- [32] Petrovic J, Langer N, Yoon S C and Heger A 2005 astro-ph/0504175
- [33] Watts A L and Andersson N 2002 *MNRAS* **333** 943
- [34] Hillebrandt W, Wolff R G and Nomoto K 1984 *Astrophys. J.* **133** 175
- [35] Liu Y T and Lindblom L 2001 *MNRAS* **324** 1063
- [36] Fryer C L, Holz D E, Hughes S A 2002 *Astrophys. J.* **565** 430
- [37] Yoon S C and Langer N 2005 astro-ph/0502133
- [38] Middleditch J 2004 *Astrophys. J.* **601** L167
- [39] Woosley S E 1993 *Bulletin of the American Astronimical Society* **25** 894
- [40] Gaensler B M et al. 2005 *Nature* **434** 1104
- [41] Fryer C L, Holz D E,Hughes S A 2004 *Astrophys. J.* **609** 288

- [42] Zwerger T, Müller E 1997 *A & A* **320** 209
- [43] Rampp M, Müller E and Ruffert M 1998 *A& A* **332** 969
- [44] Ott C D, Burrows A, Livne E, Walder R, 2004 *Astrophys. J. Lett.* **625**, 119
- [45] Burrows A, Dessart L, Livne E, Ott C D, Murphy J 2007, *Astrophys. J.* **664**, 416
- [46] Ott, C. D.; Dimmelmeier, H.; Marek, A.; Janka, H.-T.; Hawke, I.; Zink, B.; Schnetter, E. 2007, *Phys. Rev. Lett.* **98** 261101
- [47] Dimmelmeier, H.; Ott, C. D.; Janka, H.-T.; Marek, A.; Müller, E. 2007, *Phys. Rev. Lett.* **98** 261101
- [48] Ott C D, Dimmelmeier H, Marek A, Janka, H.-T, Zink B, Hawke I, Schnetter E 2007, *CQG* **24** 139
- [49] Kotake K, Yamada S and Sato K, 2003 *Phys. Rev. D* **68** 044023
- [50] Müller E, Rampp M, Buras R, Janka H-Th and Shoemaker D H 2004 *Astrophys. J.* **603** 221
- [51] Shibata M and Sekiguchi Y 2004 *Phys. Rev. D* **69** 084024
- [52] Shibata M and Sekiguchi Y 2005 *Phys. Rev. D* **71** 044017
- [53] Sekiguchi Y and Shibata M 2005 *Phys. Rev. D* **71** 084013
- [54] Andersson N, Kokkotas K D 1996 *Phys. Rev. Lett.* **77** 4134
- [55] Andersson N, Kokkotas K D 1998 *M.N.R.A.S.* **299** 1059
- [56] Epstein R 1978 *Astrophys. J.* **223** 1037
- [57] Burrows A and Hayes J 1996 *Phys. Rev. Lett.* **76** 352
- [58] Müller E and Janka H T 1997 *Astron. Astrophys.* **317** 140
- [59] Hoefflich P, Khokhlov A, Wang L, Wheeler J C and Baade D 2002, IAU Symposium 212 on Massive Stars, D. Reidel Conf. Series, ed. E. van den Hucht, astro-ph/0207272
- [60] Laarakkers W G and Poisson E 1999 *Astrophys. J.* **512** 282
- [61] Nakamura T 1981 *Prog. Theor. Phys.* **65** 1876
- [62] Stark R F and Piran T 1985 *Phys. Rev. Lett.* **55** 891
- [63] Baiotti L, Hawke I, Rezzolla L and Schnetter E 2005 *Phys. Rev. Lett.* **94** 131101
- [64] Echeverria E 1980 *Phys. Rev. D* **40** 3194
- [65] Finn L S 1992 *Phys. Rev. D* **8** 3308
- [66] Nakano H, Takahashi H, Tagoshi H and Sasaki M 2003 *Phys. Rev. D* **68** 102003
- [67] Dryer O, Kelly B, Krishnan B, Finn L S, Garrison D, Lopez-Aleman R 2004 *Class. Quantum Grav.* **21** 787
- [68] Davis M, Ruffini R, Press W H and Price R H 1971 **27** 1466
- [69] Shibata M, Baumgarte T W and Shapiro S L 2000 *Astrophys. J.* **542** 453
- [70] Saijo M, Shibata M, Baumgarte T W and Shapiro S L 2001 *Astrophys. J.* **548** 919
- [71] Centrella J M , New K C B., Lowe L L , Brown J D 2001 *Astrophys. J. Lett.* **550** 193
- [72] Shibata M, Karino S, Eriguchi Y 2002 *MNRAS* **334** L27
- [73] Shibata M, Karino S, Eriguchi Y 2003 *MNRAS* **343** 619
- [74] Saijo M, Baumgarte T W and Shapiro S L, 2002 *Astrophys. J* **595** 352
- [75] Saijo M and Yoshida Y 2006 *MNRAS* **368** 1429
- [76] Watts A L, Andersson N and Williams R L 2004 *MNRAS* **350** 927
- [77] Passamonti A, Stavridis A, Kokkotas KD 2008 *Phys. Rev. D* in press , gr-qc/0706.0991
- [78] Ott C D, Ou S, Tohline J E, Burrows A 2006 *Astroph. J. Lett.* **625**, 119
- [79] Chandrasekhar S 1970 *Phys. Rev. Lett.* **24** 611
- [80] Friedman J L and Schutz B F 1978 *Astrophys. J.* **222** 281
- [81] Cutler C and Lindblom L 1987 *Astrophys. J.* **314** 234

- [82] Lindblom L and Detweiler S 1979 *Astrophys. J.* **232** L101
- [83] Ipser J R and Lindblom L 1991 *Astrophys. J.* **373** 213
- [84] Lindblom L and Mendell G 1995 *Astrophys. J.* **444** 804
- [85] Stergioulas N, Friedman J L, 1998 *Astrophys. J.* **492** 301
- [86] Morsink S, Stergioulas N and Blattning S 1999 *Astrophys. J.* **510** 854
- [87] Liu Y T and Shapiro S L 2004 *Phys. Rev. D* **69** 044009
- [88] Yoshida S, Rezzolla L, Karino S and Eriguchi Y, 2002 *Astrophys. J. Lett.* **568** 41
- [89] Lai D and Shapiro S L 1995 *Astrophys. J.* **442** 259
- [90] Shibata M and Karino S 2004 *Phys. Rev. D* **70** 084022
- [91] Ou S, Tohline J E and Lindblom L 2004 *Astrophys. J.* **617** 490
- [92] Lifschitz A and Lebovitz N 1993 *Astrophys. J.* **408** 603
- [93] Andersson N 1998 *Astrophys. J.* **502** 708
- [94] Friedman J L and Morsink S 1998 *Astrophys. J.* **502** 714
- [95] Linblom L, Owen B J and Morsink S M 1998 *Phys. Rev. Lett.* **80** 4843
- [96] Andersson N, Kokkotas K D and Schutz B F 1999 *Astrophys. J.* **510** 846
- [97] Lindblom L, Owen B, 2002 *Phys. Rev. D* **65** 063006
- [98] Rezzolla L, Lamb, F K, Markovic D and Shapiro S L 2001 *Phys. Rev. D* **64** 104013
- [99] Rezzolla L, Lamb, F K, Markovic D and Shapiro S L 2001 *Phys. Rev. D* **64** 104014
- [100] Andersson N and Kokkotas K D 2001 *Int. J. Modern Phys.* **D10** 381
- [101] Andersson N 2003 *Class. Quantum Grav.* **20** R105
- [102] van Dalen E N E and Dieperink A E L 2003 *Phys. Rev. C* **69** 025802
- [103] Nice, D. J., Splaver, E. M., Stairs, I. H., 2003, astro-ph/0311296
- [104] Schenk A K, Arras P, Flanagan E E, Teukolsky S A, Wasserman I 2002 *Phys. Rev. D* **65** 024001
- [105] Sa P M 2004 *Phys. Rev. D* **69** 084001
- [106] Sa P M and Tome B 2005 *Phys. Rev. D* **71** 044007
- [107] Bondarescu R, Teukolsky S A and Ira Wasserman I 2007 *Phys. Rev. D.* **76** 064019
- [108] Stergioulas N and Font J A 2001 *Phys. Rev. Lett.* **86** 1148
- [109] Gressman P, Lin L M, Suen W M, Stergioulas N and Friedman J L 2002 *Phys. Rev. D.* **66** 041303(R)
- [110] Lin L M and Suen W M 2004 gr-qc/0409037
- [111] Brink J, Teukolsky S A and Wasserman I 2004 *Phys. Rev. D.* **70** 121501
- [112] Brink J, Teukolsky S A and Wasserman I 2004 *Phys. Rev. D.* **70** 124017
- [113] Brink J, Teukolsky S A and Wasserman I 2005 *Phys. Rev. D.* **71** 064029
- [114] Andersson N, Jones D I and Kokkotas K D 2002 *MNRAS* **337** 1224
- [115] Lai D 1999 *MNRAS* **307** 1001
- [116] Kokkotas K D, Ruoff J and Andersson N 2004 *Phys. Rev. D* **70** 043003
- [117] Roberts P H and Stewartson K 1963 *Astrophys. J.* **137** 777
- [118] Bildsten L. 1998 *Astrophys. J.* **501** L89
- [119] Wagoner R.V., 1984 *Astrophys. J.* **278** 345
- [120] Papaloizou J., Pringle J.E., 1978 *MNRAS* **184**, 501
- [121] Andersson N, Kokkotas K D and Stergioulas N 1999 *Astrophys. J.* **307** 314
- [122] Levin Y., 1999 *Astrophys. J.* **517** 328
- [123] Andersson N, Jones D I, Kokkotas K D and Stergioulas N 2000 *Astrophys. J. Lett.* **534** 75
- [124] Heyl J 2002 *Astrophys. J. Lett.* **574** L57

- [125] Madsen J., 1998 *Phys. Rev. Lett.* **81**, 3311
- [126] Wagoner R V 2002 *Astrophys. J. Lett.* 578 L63
- [127] Reisenegger A., Bonacic A., 2003 *Phys. Rev. Lett.* **91** 201103
- [128] Benhar O, Berti E and Ferrari V 1999 *MNRAS* **310** 797
- [129] Kokkotas K D, Apostolatos T, Andersson N 2001 *M.N.R.A.S.* **320** 307
- [130] Sotani H, Kohri K and Harada T 2004 *Phys. Rev. D* **69** 084008
- [131] Sotani H and Kokkotas K D 2004 *Phys. Rev. D* **70** 084026
- [132] Benhar O, Ferrari V and Gualtieri L 2004 *Phys. Rev. D* **70** 124015
- [133] Andersson N and Comer G L 2001 *Phys. Rev. Lett.* **87**, 241101
- [134] Stergioulas N, Apostolatos T A and Font J A 2004 *MNRAS* **352**, 1089